Bull. Mater. Sci., Vol. 35, No. 4, August 2012, pp. 623–629. © Indian Academy of Sciences.

Growth, characterization and transport properties of $Pb_xZn_{1-x}S$ mixed crystals

M NAGABHUSHANA*, E NAGABUSHAN †, D JAYA PRAKASH†, B RAJAM† and K YADAIAH‡

Department of Physics, University College of Science, Osmania University, Hyderabad 500 007, India
†University College of Technology, Osmania University, Hyderabad 500 007, India
‡S.V.Degree and P.G.College, Nalagonda (Dist), Suryapeta 508 213, India

MS received 1 May 2008

Abstract. **The polycrystalline $Pb_xZn_{1-x}S$ semiconductor powder with ($0 \leq x \leq 0{\cdot}5$) has been prepared by controlled co-precipitation method from an alkaline medium using thiourea as a sulphide ion source. Pellets are made with these powders applying 10 ton/sq cm pressure and sintered at 800 °C for 2 h in nitrogen atmosphere. X-ray studies of these samples have indicated that the compounds are polycrystalline in nature with mixed hexagonal and cubic structure of ZnS and cubic structure of PbS. Lattice parameters (a and c) of all the compounds are determined from the X-ray data and are found to decrease non-linearly with increase in Pb concentration (x). It is also observed that the grain size of the crystallites increases in samples with $x = 0$–$0{\cdot}5$. Scanning electron micrographs have shown that both cubic and hexagonal crystallites are present in the mixed crystals. The electrical conductivity in $Pb_xZn_{1-x}S$ is found to decrease with increase in composition ($x = 0$–$0{\cdot}5$), whereas it increases at all temperatures in all samples. Mobility of charge carrier concentration is found to increase with increasing temperature. The increase in carrier mobility in $Pb_xZn_{1-x}S$ samples may be due to reduced grain boundary potential. In $Pb_xZn_{1-x}S$ samples with $x = 0$–$0{\cdot}3$, sum of the activation energy due to charge carriers and grain boundary potential is equal to the activation energy due to conductivity.**

Keywords. **Growth; semiconductors; $Pb_xZn_{1-x}S$ mixed crystals; co-precipitation methods; crystal structure; activation energy.**

1. Introduction

Solid solutions of group II–VI compounds such as $Pb_xZn_{1-x}S$ formed out of PbS and ZnS have considerable technological importance due to their semiconducting nature. These multicomponent materials and their alloys have potential applications in the field of electric, electro optical, photoconductive and photovoltaic devices. PbS and ZnS exist in two polymeric modifications either in hexagonal (H) of wurtzite (W) or cubic (C) in zincblende (ZB) structure. Thin films of such binary and ternary semiconductors have been prepared by evaporation, sputtering, spray pyrolysis and electrodeposition. But out of all these, chemical deposition has been successfully used to prepare a large number of semiconductor thin films such as CdSe (Kainthla *et al* 1980, 1983; Rajeshwar *et al* 1981), CdS (Kaur *et al* 1980), PbSe (Kainthla *et al* 1980). These materials have applications in photovoltaic, photoconducting cells and other electro-optical devices. Solid solutions or alloys of semiconductors are of particular interest due to the possibility of tailoring their properties to meet specific requirements in the device fabrication. However, increasing interest in semiconducting solutions based on group IV–VI compounds is due to a number of reasons. On the other hand, solid solutions are promising materials for electronic technology (Bari *et al* 2007; Harman and Melnagailis 1974), which created considerable practical importance. On the other hand, narrow gap semiconductors exhibit unique properties such as a strong dependence of the energy gap (E_g) on the composition and temperature. The development of technology of $Pb_xZn_{1-x}S$ and $PbS_{1-x}Se_x$ solid solutions is related to the wide use of these materials in infrared techniques. In view of the specific properties of semiconductor with small and controlled energy gap, very small effective masses, high carrier mobilities, anomalous values of the dielectric constant etc are widely investigated.

ZnS and PbS exist in two polymorphic modifications, either in hexagonal or cubic structure. Hence, there may be a composition of $Pb_xZn_{1-x}S$ for which the structure changes from hexagonal to cubic. PbS is known to form different types of ternary chalcogenide semiconductors. For example, addition of PbS and GeS–GeS_2 glass forming system yields new types of amorphous semiconductors over a wide range of compositions (Feltz and Voigt 1974). PbS, GeS–GeS_2 and $Pb_{1-x}Sn_xTe$ thin films find extensive applications in semiconductor device technology (Andrcos *et al* 1972; Kapon and Katzir 1985). Most of the work reported on this material is confined to the x value of 0·2 owing to its wide applications in IR detector in the 8–14 μm atmospheric window region (Melngailis and Hermann 1970). Though some structural and electrical studies on PbS films are reported, limited studies

*Author for correspondence (enaaaga@yahoo.com)

on $Pb_xZn_{1-x}S$ pellets are carried out and investigations on solid solutions of bulk nature are not reported. Therefore, the aim of the present work has been to study the optical, electrical and structural properties of bulk $Pb_xZn_{1-x}S$ mixed crystals with $x = 0$–$0{\cdot}5$. $Pb_xZn_{1-x}S$ powder was prepared by controlled precipitation method using thiourea as a sulphide-releasing source. The precipitate of mixed metal sulfide obtained from co-precipitation method was presintered in nitrogen atmosphere. Pellets of the powder are sintered again in nitrogen atmosphere at an elevated temperature. The samples showed low resistivity of few ohms. The pellets were characterized using XRD, SEM, chemical analysis, optical and electrical studies and the results are explained on the basis of different phases formed in the material.

2. Experimental

$Pb_xZn_{1-x}S$ powder was prepared by controlled precipitation method. In this method, equimolar solutions of lead acetate, zinc acetate and thiourea were taken in different compositions. The solution mixture was made alkaline by adding 25% of liquid ammonia under a constant stirring process. The solution was heated at about 80 °C (± 2) with a constant stirring process for 45 min. The colour of the solution changed from yellow to grey as 'x' varied from 0 to 1, indicating the starting of precipitation. The bath was heated further for 3 h to complete the reaction. The precipitate was filtered through Whatman filter no. 41 and was rinsed with double distilled water repeatedly. The precipitate was then collected and dried at room temperature for 24 h. The dried precipitate was transferred into a clean and dry quartz boat and was kept in a quartz tube of diameter 3 cm and length 1 cm, arranged in a high temperature (0–1000 °C) tubular furnace. Both the ends of quartz tube were provided with two metal caps to pass inert gas through the tube. The precipitate was heated in nitrogen atmosphere for 2 h at 300 °C and then cooled to room temperature. This was ground to fine powder and the process was repeated in order to obtain uniform particle size. The powder was made into pellets under pressure by using a punch die of 1·5 cm diameter. The hydraulic pressure applied for pellet formation was 10 tons per sq. cm. and for a duration of 10 min. Fixed amount of powder was taken so that the pellets have nearly 1 mm thickness. The pellets were heated at 800 °C for 2 h in nitrogen atmosphere. The pressure of the gas was maintained uniform throughout the heating process and the furnace was cooled very slowly (10 °C/min) to room temperature. X-ray diffractograms of the samples were obtained with an XD-610 Shimadzu diffractometer. Scanning electron micrographs (SEM) were taken by the micrograph model No. Jeol-JSM-5410 LV.

A four-probe technique was used to perform electrical conductivity studies by using high grade Eltecks 1228C conducting silver paste for electrical contacts. A Keithley nano voltmeter model 182 was used to measure potential drop across the sample and Keithley multimeter Model 2000 was used to measure output of the temperature sensor (copper-constant thermocouple). A Keithley constant current source model No. 224 was used to pass constant current through the sample.

3. Results and discussion

3.1 *Growth of samples*

Bulk polycrystalline samples of $Pb_xZn_{1-x}S$ are prepared by the decomposition of thiourea in an alkaline solution containing lead and zinc salts. The preparation process is based on the slow release of Pb^{2+}/Zn^{2+} and S^{2-} ions in solution. The ions condensed on an ion–ion basis in the solution. The slow release of Pb^{2+}/Zn^{2+} ions is achieved by the dissociation of a complex species of Pb/Zn such as tetra amine lead II / tetra amine zinc II complex ion $[Pb(NH_3)_4]^{2+}/[Zn(NH_3)_4]^{2+}$. S^{2-} ions are supplied by the decomposition of an organic sulfur containing compounds, such as thiourea. $Pb_xZn_{1-x}S$ precipitate was formed by controlled precipitation method. The S^{2-} ion, released from thiourea, in alkaline medium reacts with Pb^{2+} and Zn^{2+} ions and $Pb_xZn_{1-x}S$ precipitate is formed as per the following reaction.

$$x[Pb(NH_3)_4]^{2+} + (1-x)[Zn(NH_3)_4]^{2+} + SC(NH_2)_2 \xrightarrow{NH_4OH} Pb_xZn_{1-x}S + 6NH_3 + CO_3^{2-} + H_2O. \quad (1)$$

The complex formed with 1 M concentration of $[Pb(NH_3)_4]^{2+}$, $[Zn(NH_3)_4]^{2+}$, thiourea and triethanolamine solution with ammonia gives controlled number of ions of

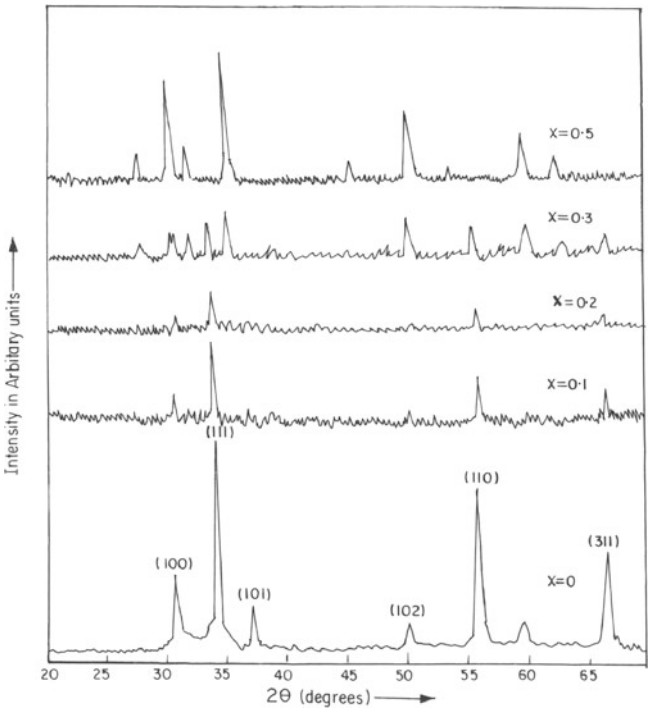

Figure 1. X-ray diffractograms of $Pb_xZn_{1-x}S$ samples with $x = 0$, 0·1, 0·2, 0·3 and 0·5.

Pb^{2+} and Zn^{2+} in which they combine with S^{2-} ions to form $Pb_xZn_{1-x}S$ powder.

3.2 *X-ray diffraction studies*

The crystallographic studies of $Pb_xZn_{1-x}S$ powder was carried out using XRD technique. Figure 1 shows X-ray diffractograms of samples $Pb_xZn_{1-x}S$ with $x = 0$–$0{\cdot}5$. The d values corresponding to the observed diffraction peaks were computed and assigned the Miller indices by comparing them with JCPDS–ICDD values of PbS and ZnS with hexagonal and cubic phases. The nature of XRD pattern indicated that the compounds were polycrystalline. One could understand that both cubic and hexagonal phases were present in $Pb_xZn_{1-x}S$ mixed crystals. Strongest peaks observed in ZnS were corresponding to $d = 3{\cdot}123$ Å and $1{\cdot}911$ Å indexed as (111) of cubic and (110) of hexagonal phases, respectively. Apart from these, other peaks assigned to ZnS are (100 H), (102 H), (220 C) and (311 C). It is observed that the peak intensities of all X-ray diffraction peaks decreased with increase in Pb concentration in the range $x = 0$–$0{\cdot}3$ and increased in sample with $x = 0{\cdot}5$ and also a small change in angular position of the peaks occurred leading to small change in lattice parameters. In samples with $x = 0{\cdot}5$, the positions of some peaks matched with PbS (C) and some with ZnS(H). No peak of ZnS(C) exists in sample with $x = 0{\cdot}5$. The highest intensity peak of XRD pattern matches with $d = 3{\cdot}0155$ spacing of PbS (C) corresponding to (h k l) values (2 0 0). The altered lattice parameters for different compositions of $Pb_xZn_{1-x}S$ ($x = 0$–$0{\cdot}5$) are calculated using X-ray data. The graphical variation of lattice parameters a and c for $0 \leq x \leq 0{\cdot}5$ are shown in figures 2 and 3, respectively. It may be noted from the figure that a and c parameters decrease non-linearly with lead concentration (x). The non-linear variation of 'a' with x are related with the values of 'a' obtained for ZnS, PbS and a bowing parameter, b, as

$$A_x = a_{ZnS}(a_{PbS} - a_{ZnS} + b)x - bx^2. \tag{2}$$

The samples undergo a crystalline transition from ZnS (C) to PbS (C). The lattice parameter thus determined for samples with $x = 0$–$0{\cdot}5$ decreased and matched with the reported value of ZnS with cubic structure, and more number of peaks were observed when compared with those reported by other workers (Kowk and Siu 1979).

3.3 *Scanning electron microscope studies*

Figures 4(a–d) represent the scanning electron micrographs of $Pb_xZn_{1-x}S$ pellets with $x = 0$–$0{\cdot}5$. It is evident from the

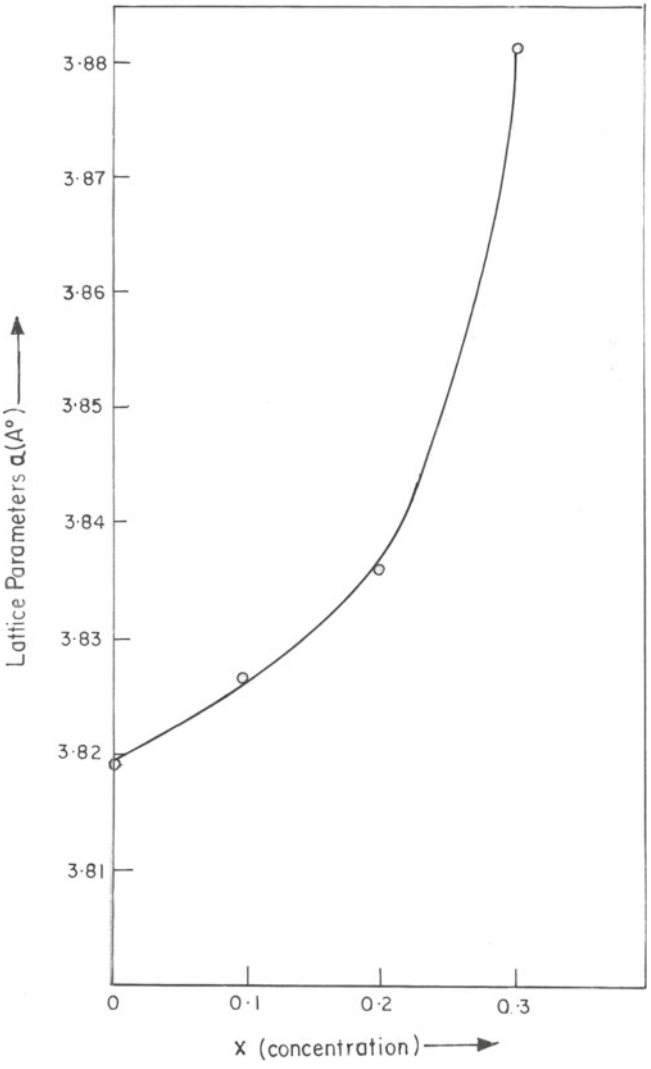

Figure 2. Variation of lattice parameter a (Å) of $Pb_xZn_{1-x}S$ with $x = 0$ to $0{\cdot}3$.

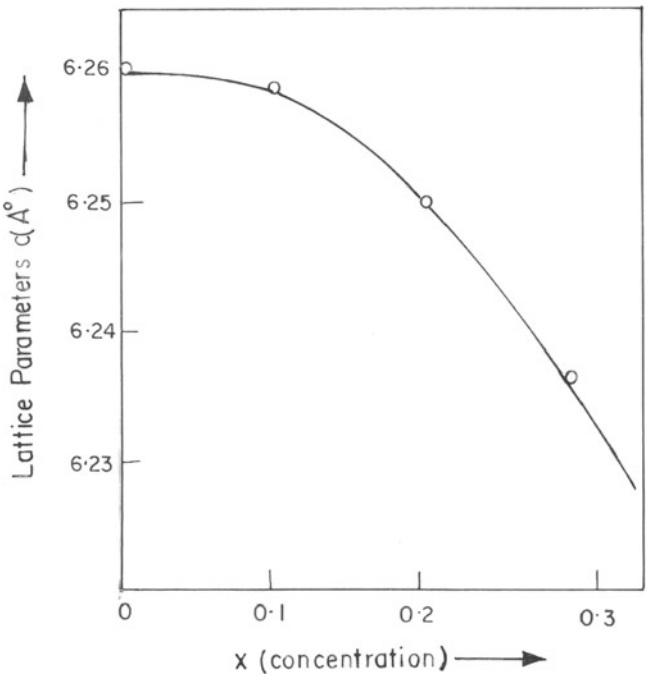

Figure 3. Variation of lattice parameter c (Å) of $Pb_xZn_{1-x}S$ with $x = 0$ to $0{\cdot}3$.

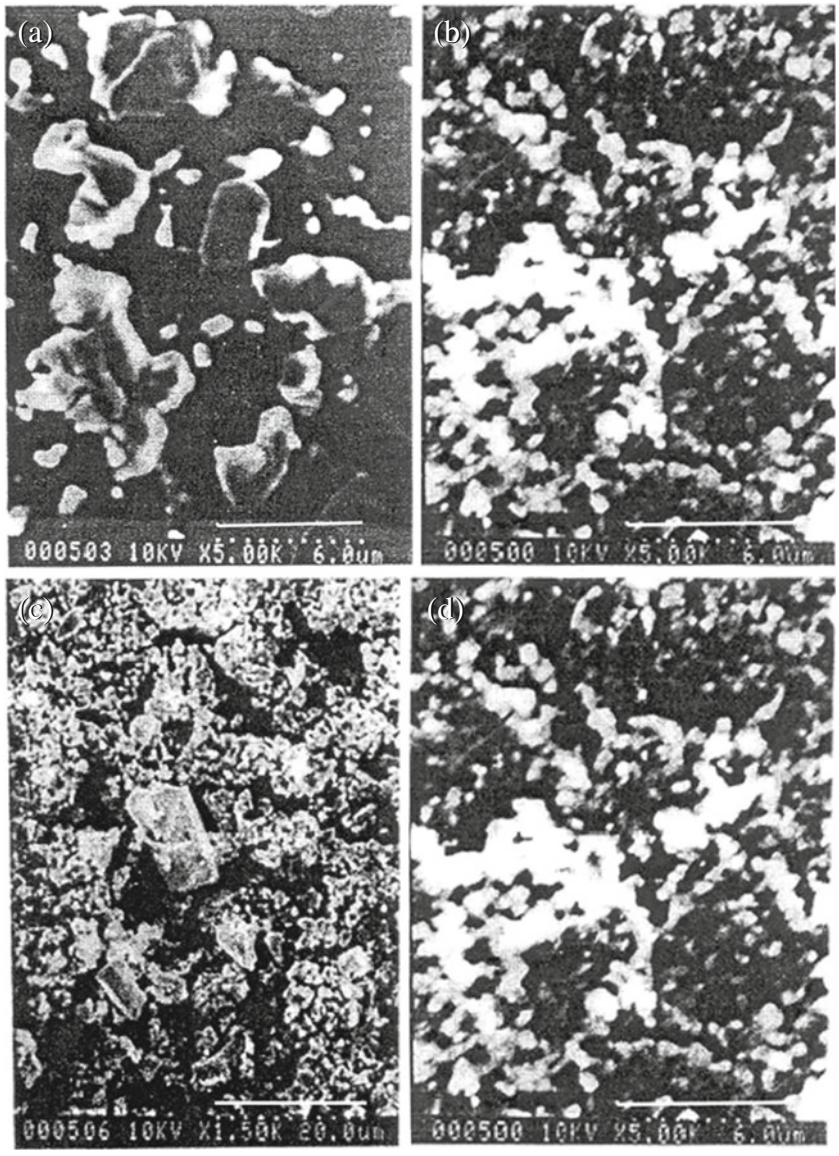

Figure 4. SEM photographs of Pb_xZn_{1-x} sample with (**a**) $x = 0$, (**b**) $x = 0{\cdot}1$, (**c**) $x = 0{\cdot}3$ and (**d**) $x = 0{\cdot}5$.

micrographs that the structure of the crystals (hexagonal) appearing in $Pb_{0{\cdot}5}Zn_{0{\cdot}5}S$ pellets is shown clearly under high magnification (figure 4(d)). It is also clear from the micrographs that both cubic and hexagonal crystallites are present in the mixed crystals and size of the crystallites increases with variation of $x = 0$–$0{\cdot}5$.

3.4 *Electrical conductivity*

The variation of conductivity of $Pb_xZn_{1-x}S$ samples ($x = 0$–$0{\cdot}5$) with temperature is observed. A typical graph of the same with $x = 0{\cdot}3$ is shown in figure 5. It is observed that the conductivity increases with increase in temperature. The order of magnitude of the conductivity changes from 10^{-3} to 10^{-1} $(\Omega.\text{cm})^{-1}$ when the temperature varies from room temperature to higher temperature. The temperature dependence of conductivity is expressed by the equation

$$\sigma = \sigma_0 \exp(-E/kT), \tag{3}$$

where E is the activation energy of the defects causing conductivity. A decrease in conductivity with an increase in composition parameter x has also been observed. This may be related to the increase in bandgap and disorder structure of the sample as a result of introduction of Pb into the lattice of ZnS. As the preparation procedure involves co-precipitation of Zn and Pb, an increasing amount of Pb content in $Pb_xZn_{1-x}S$ samples leads to an increase in the creation of sulphur vacancies in the structure and causes change in the conductivity. The activation energies of conductivity for all the samples have been calculated from the linear

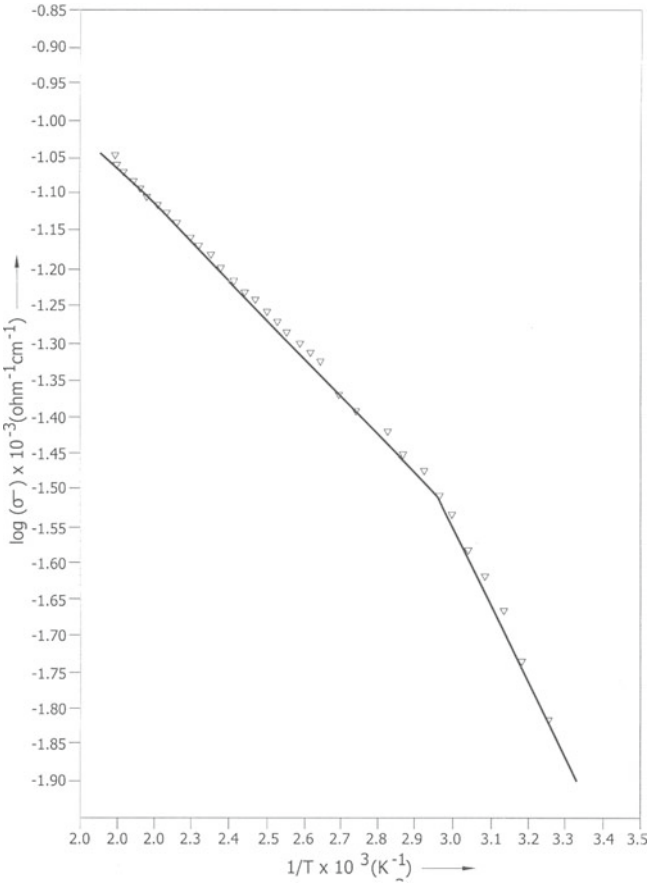

Figure 5. Variation of $\log(\sigma)$ vs $10^3/T$ of $Pb_{0.3}Zn_{0.7}S$ compound.

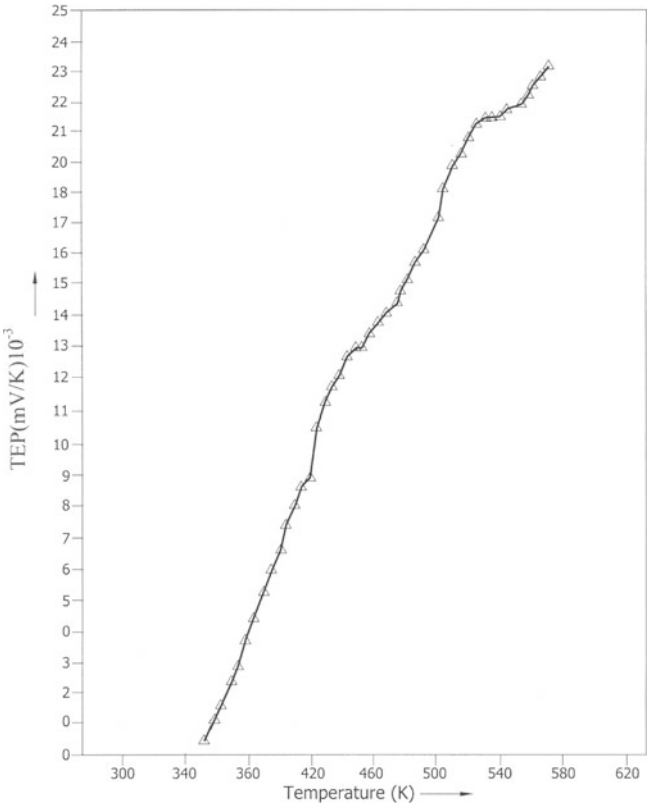

Figure 6. Variation of TEP vs T of $Pb_{0.3}Zn_{0.7}S$ compound.

portion of log σ vs $10^3/T$ graph. It is observed that the conductivity activation energy (E) is lower at low temperature levels whereas it is higher at higher temperatures.

3.5 *Thermoelectric power (TEP)*

The thermo emf measurements have been carried out on these samples by establishing temperature gradient across the thickness of the sample and by measuring the open circuit voltage. The temperature dependence of TEP of $Pb_xZn_{1-x}S$ with $x = 0{\cdot}3$ is shown in figure 6. In all the samples, thermo emf is found to be positive which indicates that they have p-type semiconductor nature. At a given temperature, magnitude of TEP increases with the increase in Pb content (in the low temperature range) and is linear and deviates at higher temperature where it obeys power law dependence of temperature. The related TEP equation is given as (Ravich *et al* 1968)

$$P = \frac{K}{e}\left[\left(r + \frac{5}{2}\right) + \ln 2\left(\frac{2\pi m_d kT}{nh^3}\right)\right], \tag{4}$$

where $r + 5/2 = A$, is the thermoelectric factor, which depends on various scattering mechanisms, m_d the density of state effective mass and n the carrier density. Solving the above equation we can write the equation for the carrier concentration as

$$\log n = 3/2 \log T - 0{\cdot}005(\text{TEP}) + 15{\cdot}718. \tag{5}$$

The carrier concentration is then calculated from the above relation. The observed carrier concentration is of the order of 10^{19} cm^{-3}. Figure 7 shows the variation of log n vs $10^3/T$ of Pb_x $Zn_{1-x}S$ with $x = 0{\cdot}1$. The plots exhibit two regions showing two conduction mechanisms. The activation energies of electron density (E_{an}) in both the regions have been determined. In the low temperature region, the calculated activation energies are 0·04460, 0·03966, 0·04480 and 0·03800 eV, whereas in the higher temperature regions they are 0·04938, 0·04628 and 0·42100 eV. Further the data is analysed by obtaining the charge carrier mobility using the relation

$$\mu = \sigma/(ne). \tag{6}$$

It is observed that the mobility increases with rise in temperature, in all the samples and the increase of mobility shows two different temperature regions (i.e., lower and higher) suggesting that the electrical transport properties of $Pb_xZn_{1-x}S$ samples are governed by the scattering mechanism associated with intergrain barrier height (Peritz 1956). Further the mobility in such cases is activated by temperature and obeys exponential behaviour as

$$\mu = \mu_0 T^{-1/2} \exp(-\varphi_B/kT), \tag{7}$$

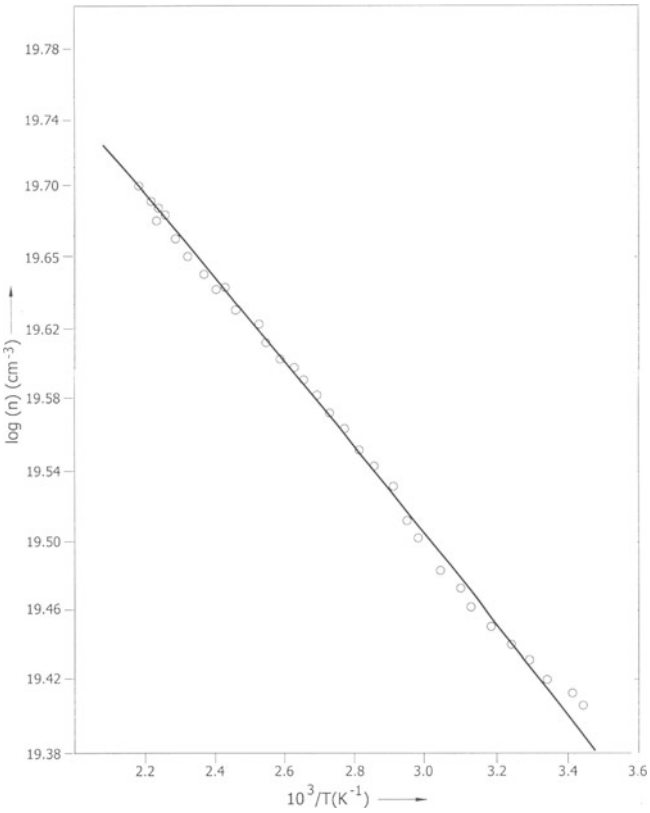

Figure 7. Variation of carrier concentration (n) vs $10^3/T$ of $Pb_{0.1}Zn_{0.9}S$ compound.

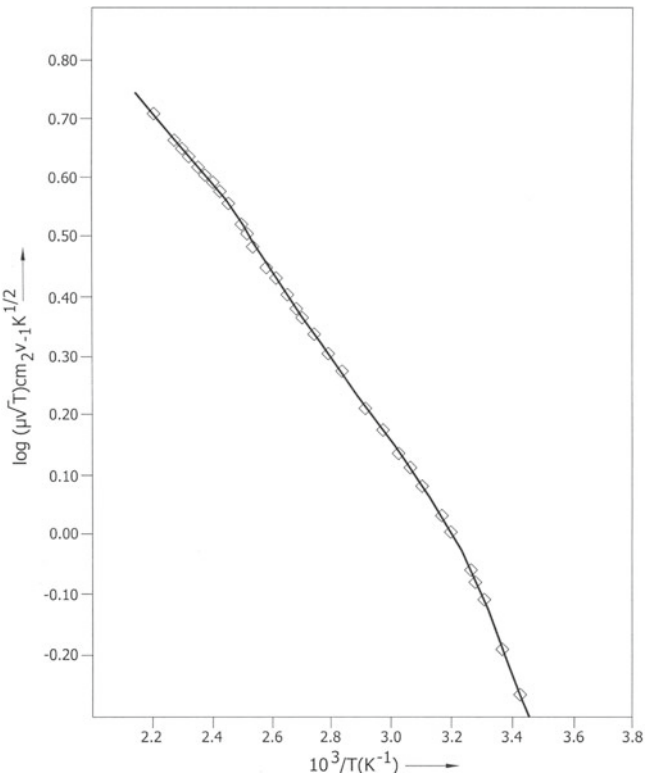

Figure 8. Variation of log ($\mu T^{1/2}$) vs $10^3/T$ of $Pb_{0.3}Zn_{0.7}S$ compound.

where φ_B is the height of the grain barrier potential and can be determined from the slope of the variation of log ($\mu T^{1/2}$) vs $1/T$ (figure 8). The height of the grain barrier potential corresponding to both the temperature regions (lower and higher) are determined from these graphs. And μ_0 is the experimental factor, which on the assumption that the current over the barrier flows by thermo-ionic emission depends on the grain size (d) and the effective mass of electron (m^*) as

$$\mu_0 = ed/(2\pi m^* kT)^{1/2}. \quad (8)$$

From the observed values of the activation energies calculated from electrical conductivity ($E_{a\sigma 1}$, $E_{a\sigma 2}$) and electron density (E_{an1}, E_{an2}) and potential barrier heights of the grain boundaries (φ_{B1}, φ_{B2}), it may be observed that they are related with each other in two regions. The observed relation for higher temperature region is

$$E_{a\sigma 1} = E_{an1} + \varphi_{B1}. \quad (9)$$

It also satisfies a similar relation for lower temperature region,

$$E_{a\sigma} = E_{an2} + \varphi_{an2} + \varphi_{B2}. \quad (10)$$

These two above equations are expected from the inter-relationship between electrical conductivity, carrier density and mobility (Heikes and Ure 1961; Micocci *et al* 1995). A similar result was also observed (Mullik *et al* 1996).

4. Conclusions

(I) Bulk polycrystalline $Pb_xZn_{1-x}S$ mixed compounds are grown by controlled co-precipitation method. All the compounds have shown semiconducting nature, except $Pb_{0.5}Zn_{0.5}S$ compound which has shown conducting nature.
(II) Lead, zinc and sulphur contents varied systematically in $Pb_xZn_{1-x}S$ compounds.
(III) Both cubic and hexagonal phases are present in $Pb_xZn_{1-x}S$ mixed crystals.
(IV) Scanning electron micrographs show that both cubic and hexagonal crystallites are present and size increases with increase of x in the range $x = 0$–$0{\cdot}5$.
(V) The electrical conductivity in $Pb_xZn_{1-x}S$ decreased with increase in the composition ($x = 0$–$0{\cdot}5$) and at a given temperature, the conductivity increased in all samples.
(VI) Mobility and charge carrier concentration increased with increasing temperature. The increase in carrier mobility may be due to the reduced grain boundary potential.
(VII) In $Pb_xZn_{1-x}S$ samples with $x = 0$–$0{\cdot}3$, the sum of the activation energy due to charge carriers and grain boundary potential is equal to the activation energy due to conductivity.

References

Andrcos A M, Higgins J A, Longo J F, Gertner E R and Pasko J F 1972 *Appl. Phys. Lett.* **21** 285

Bari R H, Patil L A, Soni A and Okram G S 2007 *Bull. Mater. Sci.* **30** 135

Feltz A and Voigt B 1974 *Z. Anorg. Allg. Chem.* **403** 61

Harman T and Melnagailis I 1974 *Appl. Solid State Sci.* **4**

Heikes R R and Ure R W 1961 *Thermoelectricity science and engineering* (New York: Inter Science) Ch. 3

Kainthla R C, Pandya D K and Chopra K L 1980 *J. Electrochem. Soc.* **127** 277

Kainthla R C, Mclann J F and Haneman D 1983 *Solar Energy Mater.* **7** 491

Kapon E and Katzir A 1985 *IEEE J. Quant.Electron.* **QE – 21** 1947

Kaur I, Pandya D K and Chopra K L 1980 *J. Electrochem. Soc.* **127** 943

Kowk H L and Siu W C 1979 *Thin Solid Films* **61** 249

Melngailis I and Hermann T C 1970 *Semiconductors and semimetals* (eds) R K Willardson and A C Beer (New York: Academic Press) **vol. 5**

Micocci G, Jepore A, Rella R and Sicihano P 1995 *Phys. Status Solidi* **148** 431

Mullik R N, Rothi C B, More B M, Sutrane D S, Shahane G S, Garadkar K M, Deshmukh L P and Hankare P P 1996 *J. Pure Appl. Phys.* **34** 903

Peritz R L 1956 *Phys. Rev.* **104** 1508

Rajeshwar K, Thompson L, Singh P, Kainthla R C and Chopra K L 1981 *J. Electrochem. Soc.* **128** 1744

Ravich Yu I, Efimova B A and Smirnov I A 1968 *Method of semiconductor investigation application to lead chalcogenides PbTe, PbSe, PbS* (Moscow: Nauka)